M. Merli; M. Giusto; A. Molfino; A. Bonetto; M. Rossi; S. Ginanni Corradini; F.M. Baccino; F. Rossi Fanelli; P. Costelli; M. Muscaritoli.
MuRF-1 and p-GSK3β expression in muscle atrophy of liver cirrhosis.
LIVER INTERNATIONAL. 33 (5) pp: 714-721.
DOI: 10.1111/liv.12128

MuRF-1 and p-GSK3β expression in muscle atrophy of liver cirrhosis

Manuela Merli[1], Michela Giusto[1], Alessio Molfino[2], Andrea Bonetto[3], Massimo Rossi[4], Stefano Ginanni Corradini[1], Francesco M. Baccino[3], Filippo Rossi Fanelli[2], Paola Costelli[3], and Maurizio Muscaritoli[2]

[1]Gastroenterology, Department of Clinical Medicine, Sapienza University of Rome, Italy

[2]Department of Clinical Medicine, Sapienza University of Rome, Italy

[3] Department of Experimental Medicine and Oncology, University of Torino, Italy

[4] Department of General Surgery and Organ Transplantation, Sapienza University of Rome, Italy

Address for correspondence

Maurizio Muscaritoli, MD, FACN

Department of Clinical Medicine

Sapienza University of Rome

Viale dell'Università 37, 00185 Rome, Italy

Phone: +390649972020

FAX: +390649972016

E-mail: maurizio.muscaritoli@uniroma1.it

Running title: muscle atrophy in cirrhosis

Abstract:

Background: Chronic diseases, including liver cirrhosis, are often accompanied by protein-energy malnutrition and muscle loss, which in turn negatively affect quality of life, morbidity and mortality. Unlike other chronic conditions few data are available on the molecular mechanisms underlying muscle wasting in this clinical setting.

Aims: To assess mechanisms of muscle atrophy in patients with liver cirrhosis.

Methods: Nutritional (Subjective Global Assessment [SGA] and anthropometry) and metabolic assessment was performed in 30 cirrhotic patients awaiting for liver transplantation.

Rectus abdominis biopsies were obtained intraoperatively in 22 cirrhotic patients and in 10 well-nourished subjects undergoing elective surgery for non-neoplastic disease, as a control group. Total RNA was extracted and mRNA for atrogenes (MuRF-1, Atrogin-1/MAFbx), myostatin (MSTN), GSK3β, and IGF-1 was assayed.

Results: 50% of cirrhotic patients were malnourished based on SGA, while 53% were muscle depleted according to Mid Arm Muscle Area (MAMA<5^{th} percentile). MuRF-1 RNA expression was significantly increased in malnourished cirrhotic patients (SGA B/C) vs well-nourished patients (SGA A) ($p=0.01$). The phosphorylation of GSK3β was up-regulated in cirrhotic patients with hepatocellular carcinoma (HCC) vs patients without tumor ($p<0.05$).

Conclusions: Muscle loss is frequently found in end-stage liver disease patients. Molecular factors pertaining to signaling pathways known to be involved in the regulation of muscle mass, are altered during liver cirrhosis and HCC.

Key words: Cirrhosis, skeletal muscle, sarcopenia, proteasome, ubiquitin, myostatin, IGF-1

Introduction

Protein calorie malnutrition and muscle wasting are a common finding in patients with advanced chronic liver disease (1, 2). The loss of muscle mass and strength (3) can ultimately affect patient's mobility and function (4) and, more importantly, it is associated with a greater risk of morbidity and mortality in patients with chronic liver disease (5, 6). Recently sarcopenia, which is defined as muscle atrophy and loss of muscle function (3), was shown to be associated with significantly increased post-transplant mortality in cirrhotic patients (7, 8).

The pathogenesis of muscle atrophy in cirrhotic patients is still largely unknown (9). Some authors have suggested that protein breakdown is increased, while others suggested that reduced protein synthesis is the main contributor (10, 11). Protein catabolism has been shown to be increased when these patients are following a low protein diet (12), while on the other hand, during long term refeeding, stable cirrhotic patients are capable of an efficient nitrogen retention and can increase protein synthesis (13).

In recent years the molecular mechanisms involved in the regulation of protein turnover in muscle have received great attention. A central role in muscle protein degradation has been attributed to the ubiquitin-proteasome system, which becomes hyper-activated in catabolic states associated with muscle depletion (14-16). In experimental models of muscle atrophy, messenger RNA levels of the components of the ubiquitin-proteasome system are over expressed (16-19).

Key enzymes in this process are the E3 ubiquitin ligases, which act as the substrate recognition component of the ubiquitin conjugation machinery. Among these, the two muscle ligases Atrogin-1, also known as MAFbx, and MuRF-1 have been identified to be hyper-expressed in several chronic conditions of muscle wasting such as diabetes, advanced cancer, and end-stage renal disease (3,20,21). Besides the degradative pathways, however, a down regulation of anabolic signaling might also be involved in the onset of muscle wasting. In particular, the potential role of insulin-like

growth factor-1 (IGF-1) and MSTN in the pathogenesis of chronic disease-associated muscle atrophy have gained increasing attention during recent years (22, 23).

The anabolic growth factor IGF-1 stimulates muscle protein synthesis by activating the phosphatidyl-inositol 3-kinase (PI3K)-Akt pathway. Once activated, Akt phosphorylates an increasing set of substrates, including factors that induce protein synthesis, gene transcription and cell proliferation, and that block apoptosis. Furthermore, Akt inactivates glycogen-synthase kinase 3β (GSK3β), which is known to be implicated in muscle atrophy (24, 25). Moreover, it has been proposed that signaling through the PI3K/Akt pathway also inhibits the expression of atrogin-1 and MuRF-1 preventing protein degradation (26). As IGF-1 over expression promotes muscle anabolism (27), its down regulation might contribute to a depletion of muscle mass (28).

Myostatin (MSTN), a member of the Transforming Growth Factors-β (TGF-β) superfamily, is a negative regulator of muscle mass (29) expressed by skeletal muscle, heart and fat tissue. In the MSTN gene knock-out mice, muscle mass increases three times more than in control animals, both due to muscle hyperplasia and hypertrophy (29) whereas systemic administration of MSTN in adult mice induces profound muscle and fat loss (30). An increase in MSTN activity could therefore also be involved in clinical conditions characterized by muscle wasting such as aging, denervation atrophy, or mechanical unloading (31, 32). Intracellular effects of MSTN are mediated by transcription factors belonging to the SMAD family.

Data concerning the molecular mechanism involved in muscle depletion have been reported in patients with cancer cachexia, sepsis and renal insufficiency (33) but studies in cirrhotic patients are still lacking. The only data available in this context have been produced in the experimental model of portocaval anastomosis (PCA) rats (34-37). In this model the expression of the genes regulating skeletal muscle mass together with the proliferation and differentiation of satellite cells (mononuclear precursor stem cells in skeletal muscle) has been investigated. Four weeks after PCA the expression of MSTN was found to be higher while a reduction in the expression of IGF1 and its receptor was found. Moreover, markers of cell proliferation and markers of differentiation of

satellite cells were found to be lower in PCA rats compared to controls. The authors suggested that skeletal muscle atrophy seen in PCA rats was a consequence of impaired satellite cell proliferation and differentiation mediated, in part, by higher MSTN and lower IGF-1 expression (34). In a subsequent study, the same authors found that PCA caused an enhanced proteolysis during the first two weeks, as demonstrated by the increase in mRNA of ubiquitin proteasome components, followed, in the further two weeks, by a reduced muscle protein synthesis due to an increased expression of MSTN and a lower expression of IGF1 as well as markers of satellite cell function (35). The administration of follistatin, a functional antagonist of MSTN, in the same experimental model, caused an increase in body weight, lean body mass, and muscle weight in the PCA rats to levels that were even higher than those in the control animals suggesting that an impaired skeletal muscle protein synthesis due to an increased expression of MSTN is the primary mechanism for low muscle mass in PCA rats (36).

Despite these interesting results, the PCA model may not entirely reflect the chronic nutritional and metabolic changes occurring in end-stage liver cirrhosis.

Therefore, in the present study, we investigated changes in the expression of regulators of skeletal muscle mass in muscle specimens of patients with end-stage liver disease undergoing liver transplantation.

Materials and Methods

Patients

Patients awaiting for elective Liver Transplantation (LT) for end-stage liver diseases at the Transplant Centre of Sapienza University of Rome, were considered for the study. All the patients were evaluated according to the standard protocol of our Transplant Centre. Demographic data, origin of liver disease, clinical examination and parameters of liver function were recorded. The severity of cirrhosis was classified according to Child-Pugh (38) and MELD score (39). A complete

nutritional assessment was always performed during a dedicated outpatient examination. Thirty consecutive patients undergoing LT were included in the study.

Ten patients matched for age and sex and with normal nutritional status, undergoing abdominal elective surgery for non-neoplastic disease, served as controls. The study was approved by the Ethical Committee of the University Hospital Policlinico Umberto I and a written informed consent was signed by all the participants before the enrolment.

Methods

Assessment of nutritional status

Anthropometric measurements and Subjective Global Nutritional Assessment (SGA) were used for nutritional evaluation in each patient. Body mass index (BMI) was computed as body weight (kg)/height (m^2). Body weight was measured after treatment of ascites and/or water retention, if present. In a few patients, dry weight was calculated by deducting an estimated weight for ascites and/or oedema. Mid-arm circumference (MAC, cm) was measured at the midpoint between the tip of the acromion and the olecranon process on the non-dominant side of the body by using a flexible tape measure. Triceps skin fold thickness (TSF) was also taken on the non-dominant side of the body, with the patients standing in a relaxed position, using a Harpender skinfold caliper (John Bull British Indicators Ltd., St. Albans, UK). Mid-arm muscle circumference (MAMC) and mid-arm muscle area (MAMA) were calculated using the MAC and TSF according to standard equation and MAMA below the 5^{th} percentile were identified by comparison with an age- and gender-matched population were recorded (40). Subjective global nutritional assessment (SGA) was carried out according to Detsky et al. (41) and based on the nutritional anamnesis (weight loss, dietary intake and gastrointestinal symptoms) and clinical examination (physical signs of malnutrition, such as depletion of subcutaneous fat and muscle mass) of the patients. Patients were classified as well nourished (SGA-A) and malnourished (SGA-B or -C). Furthermore, MAMA was utilized to stratify

patients with or without muscle depletion (MAMA $\leq$ 5th percentile or > 5th percentile, respectively).

Muscle samples

A biopsy specimen was obtained intraoperatively, during the initial phase of the operation, from the rectus abdominis muscle. After skin incision and dissection through the subcutaneous fat, the anterior sheet of the rectus abdominis muscle was opened with scissors and a muscle biopsy specimen weighing about 0.5 g was obtained. Small bleeding vessels were carefully controlled with ligatures and cautery after the muscle biopsy had been obtained, where after the operation continued in a routine fashion. No complications occurred from the biopsy procedure. The biopsy specimen was immediately frozen in liquid nitrogen and stored at -80 °C until analysis.

Semiquantitative RT-PCR

Total RNA was obtained using the TriPure reagent (Roche, Indianapolis, IN, USA) following the instructions provided by the manufacturer. RNA concentration was determined spectrophotometrically (SmartSpec 3000, Bio-Rad, Hercules, CA, USA) and its purity ensured by evaluating the 260/280 nm ratio. RNA integrity was checked by electrophoresis on 1.2% agarose gel, containing morpholino propanesulfonic acid (MOPS) 0.02 M and 18% formaldehyde.

IGF-1, MSTN, Atrogin-1 and MuRF-1 mRNA levels were determined by semiquantitative reverse-transcription polymerase chain reaction (RT-PCR) using the kit 'Ready-to-Go RT-PCR Beads' (Amersham Biosciences, Milano, Italy). Following manufacturer's protocol, 0.5 μg total RNA and 400 nM mixture of each couple of primers were added to a RT-PCR reaction mixture containing ~2.0 units *Taq* DNA-polymerase, 10 mM Tris-HCl pH 9.0, 60 mM KCl, 1.5 mM MgCl2, 200 μM dNTP, Moloney Murine Leukemia Virus (M-MuLV) Reverse Transcriptase, ribonuclease inhibitor and stabilizers to reach a final volume of 50μl in each reaction tube.

Primers for GAPDH, IGF-1, MSTN, Atrogin-1 and MuRF-1 were obtained according to published sequences (Table 1; Invitrogen, Milano, Italy). Retrotranscription was performed at 42°C for 30 min. Amplification was run as specified in Table 4. Positive and negative controls were performed. PCR products (GAPDH = 497bp; IGF-1 = 184bp; MSTN = 79bp; Atrogin-1 = 168bp; MuRF-1 = 225bp) were electrophoresed on 2% agarose gels and visualized by staining with ethidium bromide. A 100bp-standard DNA ladder (Fermentas, Burlington, ON, Canada) was used to estimate PCR products length. Normalization was performed according to GAPDH expression. Groups were compared in the linear range of amplification.

Western blotting

About 100 mg of rectus abdominis were homogenized in 80 mM TRIS-HCl, pH 6.8 (containing 100 mM DTT, 70 mM SDS, and 1 mM glycerol), kept on ice for 30 min, centrifuged at 15000 x g for 10 min at 4°C, and the supernatant collected. Protein concentration was assayed according to Lowry *et al*. (42) using BSA as working standard. Equal amounts of protein (30 μg) were heat-denaturated in sampleloading buffer (50 mM TRIS-HCl, pH 6.8, 100 mM DTT, 2% SDS, 0.1% bromophenol blue, 10% glycerol), resolved on a SDS-PAGE (12% polyacrilamide, 0.1% SDS) and transferred for 2h to nitrocellulose membranes (Bio-Rad, Hercules, CA, USA). Protein transfer was checked by Ponceau S staining.

The filters were then blocked with Tris-buffered saline (TBS) containing 0.05% Tween and 5% non-fat dry milk and incubated overnight with either a polyclonal anti-MSTN antibody (1:1000; Società Italiana Chimici, Roma, Italy) and raised against a synthetic peptide (aa 133-148) representing a portion of human GDF-8 encoded within exon 3 (LocusLink ID 2660), or a polyclonal antibody against phospho-GSK-3β (Ser 9, 1:1000; Cell Signaling Technology, Danvers, MA, USA), binding the ~46 kDa phosphorylated form of the kinase, or a goat anti phospho-Smad2/3 polyclonal antibody (1:200; Santa Cruz Biotechnology, Santa Cruz, CA, USA) raised against a short amino acid sequence containing phosphorylated Ser 423 and Ser 425 of Smad3 of

human origin (~55 kDa). Goat anti-rabbit (Bio-Rad, Hercules, CA, USA) or rabbit-anti-goat (Millipore, Vimodrone, MI, Italy) peroxidase-conjugated IgG were used as secondary antibodies.

The filters were then stripped by incubation in 62.5 mM Tris-HCl, pH 6.7, containing 100 mM 2-mercaptoethanol and 2% SDS for 30 min at 50° C, and reprobed with a mouse polyclonal antibody directed against tubulin (~50 kDa; Sigma, St. Louis, MO, USA) to normalize sample loading. The membrane-bound immune complexes were detected by enhanced chemiluminescence (Santa Cruz Biotechnology, USA) on a photon-sensitive film (Hyperfilm ECL; Amersham Biosciences, Milano, Italy). Bands quantification was performed by densitometric analysis with specific software (TotalLab, NonLinear Dynamics, Newcastle upon Tyne, UK).

Due to the variability in the muscle specimens size and the need of unfreezing for the extraction process the complete set of determinations could not be performed in all the patients and controls' samples.

Data analysis and presentation

Data are expressed as mean ± SD. Quantification of both RT-PCR and western blotting results was performed by densitometric analysis (TotalLab, NonLinear Dynamics, Newcastle upon Tyne, UK). Significance of the differences was evaluated by the t-test. A p value < 0.05 was considered significantly different.

Results

Patients characteristics

Demographic, clinical and nutritional characteristics of the 30 cirrhotic patients are reported in Table 2. The origin of liver disease was mainly post-viral (67%) and 13% of patients presented history of alcohol abuse. All patients were alcohol abstinent from at least 6 months before LT. Concomitant hepatocellular carcinoma (HCC) within Milan criteria (43) was present in 30% of the patients. Fifteen patients (50%) were malnourished, and sixteen patients (53%) were classified as

muscle-depleted. We also identified a sub-group of 12 patients (40%) presenting both malnutrition and muscle depletion. No differences in nutritional status and anthropometric measurements were observed between post-viral and post alcoholic cirrhotic patients. According to SGA, 7 out of the 9 patients with HCC were well-nourished (p= 0.04 vs non-HCC patients). According to MAMA 4 patients with HCC had muscle depletion (p= 0.5 vs non-HCC).

The control group included 5 males and 5 females, mean age 53±13 years, BMI 26±3 kg/m^2 without a known history of liver disease. Reasons of surgery were elective colecistectomy (3 patients), umbilical hernia (4 patients), ovary cystis (3 patients).

Parameters of molecular regulation of muscle proteins

A) m-RNA expression

This analysis was performed in 10 end-stage liver disease patients and in 4 controls. Within the 10 patients malnutrition was present in 4 patients according to SGA, while muscle depletion was observed in 6 patients according to MAMA. A diagnosis of concomitant HCC was also made in 6 out of these 10 patients. Prevalence on malnutrition and muscle depletion was similar in patients with and without HCC (p= 0.06 and p=0.43, respectively). No differences in the gene expression for MSTN, IGF-1, Atrogin-1 and MuRF-1 were observed between the patients and controls (Table 3).
When these parameters were examined in end-stage liver disease patients according to SGA, MuRF-1 RNA expression was significantly (p=0.01) increased in malnourished patients (SGA B/C) with respect to well-nourished patients (SGA A) (Figure 1). These patients were also muscle-depleted according to MAMA.
No influence of HCC on m-RNA expression for MSTN, Atrogin-1, MuRF-1, and IGF-1 was observed.

B) Protein levels

This analysis was performed in 22 end-stage liver disease patients and in 10 controls. Malnutrition was present in 13 patients according to SGA, while muscle depletion (MAMA $<5^{th}$) was observed in 13 patients. A diagnosis of concomitant HCC was also present in 5 of these patients.

Prevalence of malnutrition and muscle depletion was similar in patients with and without HCC ($p= 0.32$ and $p=0.96$, respectively).

No differences in protein levels of MSTN, p-SMAD2/3 and p-GSK-3β were observed between patients and controls (Figures 2-4). When these parameters were examined stratifying end-stage liver disease patients according to MAMA and SGA, no differences were observed (data not shown).

Influence of HCC on proteins levels was also evaluated and only p-GSK-3β was significantly ($p<0.05$) up-regulated by the presence of the tumor (Figure 5).

Post-transplant follow-up showed that malnourished and muscle-depleted patients presented a higher degree of complications. Bacterial and viral infections in post liver transplant were more frequent within these groups respect to well-nourished patients ($p=0.01$) and length of hospital stay was longer in patients with worse nutritional status and muscle depletion (based on SGA and MAMA) respect to well-nourished patients ($p=0.01$). These data confirm our previous observations (44).

Discussion

The present study shows that molecular factors pertaining to signaling pathways involved in the regulation of muscle mass, are altered in liver cirrhosis and HCC.

Our results also show that 50% of the patients in our series were malnourished according to SGA and 53% were muscle depleted according to MAMA. Muscle depletion in liver cirrhosis is a negative predictor of outcome (8), although it is noteworthy that loss of muscle volume does not necessarily indicate loss of muscle function. Recently, the prevalence of muscle atrophy was assessed by means of lumbar computed tomography scan (7) in a series of 112 cirrhotic patients evaluated for LT, with demographic characteristics similar to the patients enrolled in the present investigation. The CT-scan-measured prevalence of muscle loss (50% in men, 18% in women, average 45%) was similar to that diagnosed based on MAMA in our study.

The mechanisms contributing to muscle atrophy in advanced chronic liver disease have not been completely clarified (9). We have investigated, in cirrhotic patients undergoing surgery for elective liver transplantation, the mRNA expression of MSTN, IGF-1, and of components of the ubiquitin-proteasome degradative system, all belonging to signaling pathways involved in muscle atrophy and cachexia in several clinical conditions. To our knowledge, this is the first study investigating the possible role of these pathways in the regulation of muscle protein metabolism in cirrhotic patients.

From the overall comparison between cirrhotic patients and healthy controls, it would appear that the molecular pathways involved in the regulation of muscle mass are not altered in cirrhotic patients. A possible explanation for this finding is the limited number of patients included in the study and their heterogeneity. However, patient stratification according to their nutritional status revealed that, while no difference occurred as for Atrogin-1/MAFbx, espression, MuRF-1 mRNA levels were significantly increased in the malnourished group, suggesting that the ubiquitin-proteasome degradation may be activated above control levels, contributing to muscle depletion in

chronic liver disease. In this regard, modulations of muscle mass not associated with changes of atrogin-1 mRNA expression were previously reported in experimental models of muscle atrophy (28, 45). The results from the present study, together with the data reported in the literature, suggest that changes of muscle mass and atrogin-1 mRNA levels might not be tightly coupled. Finally, the lack of convergence in the modulation of atrogin-1 and MuRF-1 mRNA levels in the skeletal muscle of cirrhotic patients may reflect the differential regulation impinging on the two ubiquitin ligases (46).

Taking into consideration the anabolic/anticatabolic signaling pathway dependent on IGF-1, our results showed no significant changes as for IGF-1 mRNA expression or p-GSK3β levels in cirrhotic patients compared to controls, even when patients were stratified according to SGA or to the presence of HCC. These observations suggest that the IGF-1 pathway is not down-regulated in the skeletal muscle of cirrhotic patients. Furthermore, cirrhotic patients with HCC showed increased levels of phosphorylated (inactive) GSK3β. This kinase plays a crucial role in inhibiting the IGF-1 signaling. Indeed, when the IGF-1 pathway is induced, GSK3β is inactivated by an Akt-dependent phosphorylation, removing the negative regulation it exerts on molecules involved in anabolic processes such as protein synthesis. Consistently with this role, GSK3β inhibition was shown to induce a hypertrophic phenotype in cultured myotubes (25). In the present study, p-GSK3β levels were significantly higher in cirrhotic patients with HCC vs patients without HCC, in spite of comparable muscle depletion, according to MAMA. This observation is in agreement with previous data obtained in both gastric cancer patients and cachectic tumor-bearing animals (47,48). Therefore, it is possible that also in human HCC the anabolic signals are up regulated to counteract the catabolic stimuli induced by the presence of the tumor, suggesting that they might be more compelling than those resulting from end stage liver disease.

The lack of modulations of IGF-1 signaling lead us to verify if the MSTN pathway could be involved in muscle depletion in cirrhotic patients. In this regard, up-regulation of MSTN-dependent

signaling was proposed to result in increased expression of muscle-specific ubiquitin ligases (49, 50). Increased MSTN expression and bioactivity were reported in different experimental models of cancer cachexia (51,52) as well as in gastric cancer patients (48). We failed to find any differences in MSTN mRNA expression and protein levels in cirrhotic patients with respect to controls, even when stratified according to the presence of malnutrition or muscle depletion. These data are in contrast with the previous experimental evidences by Dasarathy et al., although in these studies muscle atrophy was induced in rats by portosystemic shunting a model which induces a liver dysfunction not exactly comparable to liver cirrhosis (34-37).

The creation of a porto-caval anastomosis in experimental animals induces liver atrophy without liver failure. In particular, the microscopic changes in the liver demonstrate a secondary atrophy that is not accompanied by changes in hepatic architecture (53).

Therefore the animal model of PCA mimics the situation induced in cirrhosis by porto-systemic shunting, but does not reproduce the condition of progressive liver insufficiency characteristic of this illness. It is also unclear if alterations in nutritional status and muscle depletion, which are observed in PCA rats, are determined by the same physiopathological mechanism of cirrhotic patients. In fact, the contributors of muscle depletion and malnutrition in cirrhosis are multifactorial and probably more complex.

Cirrhotic patients have a long lasting chronic liver disease, and malnutrition is a progressive and gradual manifestation associated to the more advanced stages of the disease rather than a rapid short term event. For this reason the catabolic muscle pathways may be activated in some phases during the illness but, in the same way, counteracting mechanism may also occur to avoid the development of cachexia. These circumstances may explain way the muscle molecular pathways evaluated in our study were not completely activated in malnourished cirrhotic patients.

Finally, we confirmed that muscle depleted/malnourished patients had increased post-transplant complications. Considering the well-established negative prognostic value of sarcopenia on survival

in both non-transplanted and transplanted cirrhotic patients (3,8) further clinical studies are mandatory to better explain the mechanisms underlying muscle loss in end-stage liver disease. These could allow for the development of preventative and therapeutic strategies for muscle atrophy aimed at further improving quality of life and survival in liver cirrhosis.

References

1. Merli M , Riggio O, Capocaccia L for Policentrica Italiana Nutrizione Cirrosi. Nutritional status in liver cirrhosis.. *Journal Hepatol* 1994; **21**: 317-325.

2. Caregaro L, Alberino F, Amodio P, *et al*. Malnutrition in alcoholic and virus-related cirrhosis. *Am J Clin Nutr* 1996; **63:** 602–9.

3. Muscaritoli M, Anker SD, Argilés J, *et al*. Consensus definition of sarcopenia, cachexia and pre-cachexia: joint document elaborated by Special Interest Groups (SIG) "cachexia-anorexia in chronic wasting diseases" and "nutrition in geriatrics". *Clin Nutr* 2010; **29:**154–9.

4. Álvares-da-Silva MR, Reverbel da Silveira T. Comparison between handgrip strength, subjective global assessment, and prognostic nutritional index in assessing malnutrition and predicting clinical outcome in cirrhotic outpatients. *Nutrition* 2005; **21:**113–7.

5. Merli M, Riggio O, Dally L. Does malnutrition affect survival in cirrhosis? *Hepatology* 1996; **23:** 1041–6.

6. Merli M, Nicolini G, Angeloni S, Riggio O. Malnutrition is a risk factor in cirrhotic patients undergoing surgery. *Nutrition* 2002;18:978–86.

7. Montano-Loza AJ, Meza-Junco J, Prado CM, *et al*. Muscle wasting is associated with mortality in patients with cirrhosis. *Clin Gastroenterol Hepatol* 2012; **10:** 166-73.
8. Englesbe MJ, Patel SP, He K, *et al*. Sarcopenia and mortality after liver transplantation. *J Am Coll Surg* 2010; **211:** 271–8.
9. Dasarathy S. Consilience in sarcopenia of cirrhosis. *J Cachexia Sarcopenia Muscle*. 2012 May **31** (Epub ahead of print).
10. McCullough A J, Tavill A S. Disordered Energy and protein metabolism in liver disease. *Semin Liver Dis* 1991; **11:** 265-73.
11. Tessari P. Protein metabolism in liver cirrhosis: from albumin to muscle myofibrils. *Curr Opin Clin Nutr Metab Care* 2003; **6:** 79-85.
12. Cordoba J, Lopez-Hellin J, Planas M, *et al*. Normal protein diet for episodic hepatic encephalopathy: results of a randomized study. *J Hepatol* 2004; **41:** 38 – 43.
13. Nielsen K, Kondrup J, Martinsen L, *et al*. Long-term oral refeeding of patients with cirrhosis of the liver. *Br J Nutr* 1995; **74:** 557-67.
14. Mitch WE, Goldberg AL. Mechanisms of muscle wasting. The role of the ubiquitin-proteasome pathway. *N Engl J Med* 1996; **335:** 1897-905.
15. Bossola M, Muscaritoli M, Costelli P, *et al*. Increased muscle ubiquitin mRNA levels in gastric cancer patients. *Am J Physiol Regul Integr Comp Physiol* 2001; **280:** R1518-23.
16. Ciechanover A. The ubiquitin-proteasome proteolytic pathway. *Cell* 1994; **79:** 13-21.
17. Lecker SH, Jagoe RT, Gilbert A, *et al*. Multiple types of skeletal muscle atrophy involve a common program of changes in gene expression. *FASEB J* 2004; **18:** 39-51.
18. Jagoe RT, Lecker SH, Gomes M, Goldberg AL. Patterns of gene expression in atrophying skeletal muscles: response to food deprivation. *FASEB J* 2002; **16:** 1697-712.
19. Cao PR, Hannah JK, Stewart HL. Ubiquitin–protein ligases in muscle wasting. *Int J Biochem Cell Biol* 2005; **37:** 2088–97.

20. Lagirand-Cantaloube J, Cornille K, Csibi A, *et al*. Inhibition of Atrogin-1/MAFbx Mediated MyoD Proteolysis Prevents Skeletal Muscle Atrophy In Vivo. *PLoS ONE* 2009; **4:** e4973. doi:10.1371/journal.pone.0004973.

21. Zhao W, Wu Y, Zhao J, *et al*. Structure and function of the upstream promotor of the human Mafbx gene: the proximal upstream promotor modulates tissue-specificity. *J Cell Biochem* 2005; **96:** 209-19.

22. Philippou1 A, Halapas1 A, Maridaki, M, Koutsilieris M. Type I insulin-like growth factor receptor signaling inskeletal muscle regeneration and hypertrophy. *J Musculoskelet Neuronal Interact* 2007; **7:** 208-18.

23. Kollias HD, McDermott JC. Transforming growth factor- and myostatin signaling in skeletal muscle. *J Appl Physiol* 2007; **104:** 579–87.

24. Cross DA, Alessi DR, Cohen P, Andjelkovich M, Hemmings BA. Inhibition of glycogen synthase kinase-3 by insulin mediated by protein kinase B. *Nature* 1995; **378:** 785-9.

25. Rommel C, Bodine SC, Clarke BA, *et al*. Mediation ofIGF-1-induced skeletal myotube hypertrophy by PI(3)K/Akt/mTOR and PI(3)K/Akt/GSK3 pathways. *Nat Cell Biol* 2001; **3:** 1009–13

26. Sandri M, Sandri C, Gilbert A, *et al*. Foxo transcription factors induce the atrophy-related ubiquitin ligase atrogin-1 and cause skeletal muscle atrophy. *Cell* 2004; **117:** 399–412.

27. Florini JR, Ewton DZ, Coolican SA. Growth hormone and the insulin-like growth factor system in myogenesis. *Endocr Rev* 1996; **17:** 481–517.

28. Costelli P, Muscaritoli M, Bossola M, *et al*. IGF-1 is downregulated in experimental cancer cachexia. *Am J Physiol Regul Integr Comp Physiol* 2006; **291:** R674–83.

29. McPherron AC, Lawler AM, Lee SJ. Regulation of skeletal muscle mass in mice by a new TGF-beta superfamily member. *Nature* 1997; **387:** 83–90.

30. Zimmers TA, Davies MV, Koniaris LG. Induction of cachexia in mice by systemically administered myostatin. *Science* 2002; **296:** 1486–8.

31. Baumann AP, Ibebunjo C, Grasser WA, Paralkar VM. Myostatin expression in age and denervation-induced skeletal muscle atrophy. *J Muscoskelet Neuronal Interact* 2003; **3:** 8–16.

32. Kirk S, Oldham J, Kambadur R, *et al*. Myostatin regulation during skeletal muscle regeneration. *J Cell Physiol* 2000; **184:** 356–63.

33. Aversa Z, Alamdari N, Hasselgren PO. Molecules modulating gene transcription during muscle wasting in cancer, sepsis, and other critical illness. *Crit Rev Clin Lab Sci* 2011; **48:** 71-86.

34. Dasarathy S, Dodig M, Muc SM, Kalhan SC, McCullough AJ. Skeletal muscle atrophy is associated with an increased expression of myostatin and impaired satellite cell function in the portacaval anastamosis rat. *Am J Physiol Gastrointest Liver Physiol* 2004; **287:** G1124-30.

35. Dasarathy S, Muc S, Hisamuddin K, *et al*. Altered expression of genes regulating skeletal muscle mass in the portacaval anastomosis rat. *Am J Physiol Gastrointest Liver Physiol* 2007; **292:** G1105-13.

36. Dasarathy S, McCullough AJ, Muc S, *et al*. Sarcopenia associated with portosystemic shunting is reversed by follistatin. *J Hepatol* 2011; **54:** 915-21.

37. Dasarathy S, Muc S, Runkana A, *et al*. Alteration in body composition in the portacaval anastamosis rat is mediated by increased expression of myostatin. *Am J Physiol Gastrointest Liver Physiol* 2011; **301:** G731-8.

38. Child CG III, Turcotte JG. Surgery and portal hypertension. In: Child CG, ed. The Liver and Portal Hypertension. *Philadelphia: W. B. Saunders Co*, 1964; 50–64 (2008) 531-538

39. Wiesner RH, McDiarmid SV, Kamath PS, *et al*. MELD and PELD: application of survival models to liver allocation. *Liver Transpl* 2001; **7:** 567–80.

40. Frisancho AR. New standards of weight and body composition by frame size and height for assessment of nutritional status of adults and the elderly. *Am J Clin Nutr* 1984; **40:** 808–19.

41. Detsky AS, McLaughilin JR, Baker JP, *et al*. What is subjective global assessment of nutritional status? *JPEN* 1987; **11:** 8–13.

42. Lowry O, Rosebrough NJ, Farr AL, Randall RJ. Protein measurement with the Folin phenol reagent. *J Biol Chem* 1951; **193:** 265–75.

43. Mazzaferro V, Regalia E, Doci R *et al.* Liver transplantation for the treatment of small hepatocellular carcinomas in patients with cirrhosis. *N Engl J Med* 1996; **334:** 693-9.

44. Merli M, Giusto M, Gentili F, *et al*. Nutritional status: its influence on the outcome of patients undergoing liver transplantation. *Liver Int* 2010; **30:** 208-14.

45. Fang CH, Li BG, James JH, *et al.* Protein breakdown in muscle from burned rats is blocked by insulin-like growth factor I and glycogen synthase kinase-3beta inhibitors. *Endocrinology* 2005; **146:** 3141-9.

46. Attaix D, Baracos VE. MAFbx/Atrogin-1 expression is a poor index of muscle proteolysis. *Curr Opin Clin Nutr Metab Care* 2010; **13:** 223-4.

47. Penna F, Bonetto A, Muscaritoli M, *et al*. Muscle atrophy in experimental cancer cachexia: is the IGF-1 signaling pathway involved? *Int J Cancer* 2010; **127:** 1706-17.

48. Aversa Z, Bonetto A, Penna F, *et al*. Changes in Myostatin Signaling in Non-Weight-Losing Cancer Patients. *Ann Surg Oncol* 2011; 19:1350-6.

49. McFarlane C, Plummer E, Thomas M, *et al*. Myostatin induces cachexia by activating the ubiquitin proteolytic system through an NF-kappaB-independent, FoxO1-dependent mechanism. *J Cell Physiol* 2006; **209:** 501-14.

50. Tsuchida K. Myostatin inhibition by a follistatin-derived peptide ameliorates the pathophysiology of muscular dystrophy model mice. *Acta Myol* 2008; **27:** 14-8.

51. Costelli P, Muscaritoli M, Bonetto A, *et al*. Muscle myostatin signaling is enhanced in experimental cancer cachexia. *Eur J Clin Invest* 2008; **38:** 531–8.

52. Benny Klimek ME, Aydogdu T, Link MJ, *et al*. Acute inhibition of myostatin-family proteins preserves skeletal muscle in mouse models of cancer cachexia. *Biochem Biophys Res Commun* 2010; **391:** 1548-54.

53. Butterworth RF, Noremberg MD, Felipo V, *et al*. Experimental models of hepatic encephalopathy: ISHEN guidelines. *Liver Int* 2009; **29:** 783-8.

Table 1

Oligonucleotide sequences

Gene	***Primer sequence***	***Amplification***	***Cycles***
GAPDH *(NM_002046.3)*	FW: GGTGAAGGTCGGAGTCAACG RW: CAAAGTTGTCATGGATGACC	1’ 94°C 1’ 55°C 1’ 72°C	24
IGF-1 *(NM_001111283.1)*	FW: CAGCAGTCTTCCAACCCAAT RW: CACGAACTGAAGAGCATCCA	30’’ 94°C 1’ 60°C 1’ 72°C	35
MSTN *(NM_005259.2)*	FW: TGGTCATGATCTTGCTGTAACCTT RW: TGTCTGTTACCTTGACCTCTAAAAACG	1’ 95°C 1’ 60°C 1’ 72°C	35
Atrogin-1 *(NM_058229.2)*	FW: TCACAGCTCACATCCCTGAG RW: AGACTTGCCGACTCTTTGGA	1’ 95°C 1’ 58°C 1’ 72°C	25
MuRF-1 *(NM_032588.2)*	FW: TGAGCCAGAAGTTTGACACG RW: TGATGAGTTGCTTGGCAGTC	1’ 95°C 1’ 58°C 1’ 72°C	25

Abbreviations: GAPDH: Glyceraldehyde 3-Phosphate Dehydrogenase; IGF-1: Insulin-like Growth Factor-1; MSTN: Myostatin

Table 2. Demographic, clinical and nutritional characteristics of cirrhotic patients (n=30).

Age (years)(mean ± SD)	54 ± 8
Sex (male/females) (n)	24/6
Origin of liver disease (alcoholic / viral/ others) (n)	4 /20/ 6
Concomitant HCC (>T1) (n% pts)	9 (30)
MELD score (mean ± SD)	17.2 ± 6.7
Child-Pugh class A/B/C (n)	5/11/14
Weight (kg)(mean ± SD)	72.8 ± 13.7
BMI (kg/m^2)(mean ± SD)	25.3 ± 3.6
MAMC (cm)(mean ± SD)	24.3 ± 2.6
MAMA (cm^2)(mean ± SD)	45.9 ± 9.1
SGA A/B/C (n)	15/12/3
Serum Cholesterol (mg/dl)(mean ± SD)	110 ± 58
Serum Triglycerides (mg/dl) (mean ± SD)	97 ± 61
Serum total Proteins (g/dl)(mean ± SD)	6.5 ± 1.1
Serum Albumin (g/dl)(mean ± SD)	3.7 ± 1.4

Abbreviations:

HCC: Hepatocellular Carcinoma; MELD: Model for End-stage Liver Disease; BMI: body mass index;

MAMC: mid arm muscle circumference ; MAMA: mid arm muscle area; SGA: subjective global nutritional assessment.

Table 3

Expression of mRNA by reverse semiquantitative transcription (RT-PCR) of components of the ubiquitin-proteasome pathway (MuRF-1and atrogin-1) and of IGF-1 and MSTN in end-stage liver disease patients (differences between the 2 groups are not statistically significant).

	Patients (n=10)	**Controls (n=4)**
MSTN	101 ± 19	100 ± 8
IGF-1	102 ± 30	100 ± 25
Atrogin-1	90 ± 22	100± 8
MuRF-1	101 ± 28	100 ± 40

Data (mean ± SD) are expressed as percentage of controls (C=100%).

Abbreviations: MSTN: Myostatin; IGF-1: Insulin-like Growth Factor-1

Figure legends

Figure 1. Box Plot of muscle MuRF-1 mRNA expression in muscle specimens from end stage liver disease patients according to Subjective Global Assessment (SGA) score. Data (means ± SD are expressed as percentage of the controls (C=100%).

Well-nourished (SGA A): n= 6; malnourished (SGA B-C): n= 4; * p= 0.01 Malnourished patients were also muscle-depleted according to MAMA.

Figure 2. Myostatin protein levels in muscle specimens of end stage liver disease patients.

Panel A: densitometric quantifications of myostatin protein levels normalized to GAPDH. Data expressed as means ± SD, n = 22 patients and 10 controls.

Panel B: representative western blots for myostatin and GAPDH (loading controls).

Figure 3. GSK3β protein levels in muscle specimens of end stage liver disease patients.

Panel A: densitometric quantifications of pGSK3β protein levels normalized to GAPDH. Data expressed as means ± SD, n = 22 patients and 10 controls.

Panel B: representative western blots for pGSK3β and GAPDH (loading controls).

Figure 4. pSMAD 2/3 protein levels in muscle specimens of end stage liver disease patients.

Panel A: densitometric quantifications of pSMAD 2/3 protein levels normalized to GAPDH. Data expressed as means ± SD, n = 22 patients and 10 controls.

Panel B: representative western blots for pSMAD 2/3 and GAPDH (loading controls).

Figure 5. Box Plot of muscle p-GSK3β in muscle specimens from end stage liver disease patients according to the presence of Hepatocellular Carcinoma (HCC). Data (means ± SD) are expressed as percentage of controls (C=100%) (HCC n= 5, No-HCC n =17; * p =0.04).

Fig.1.

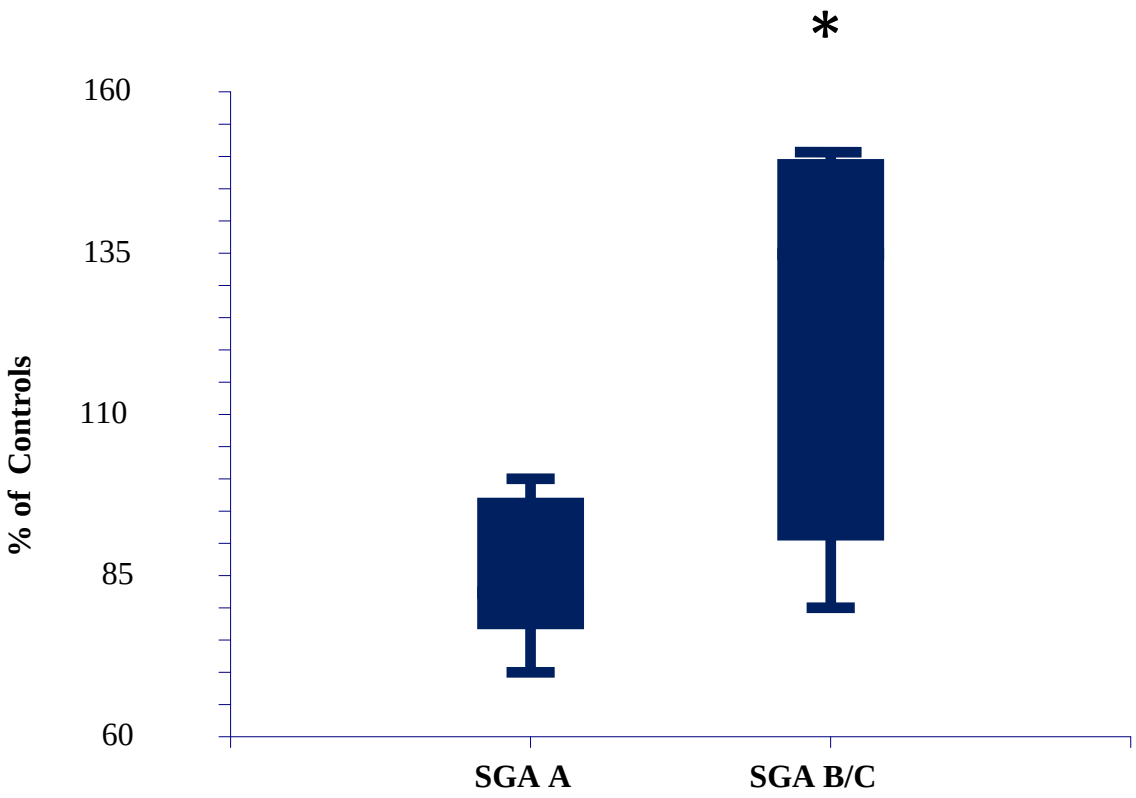

Fig.2.

A

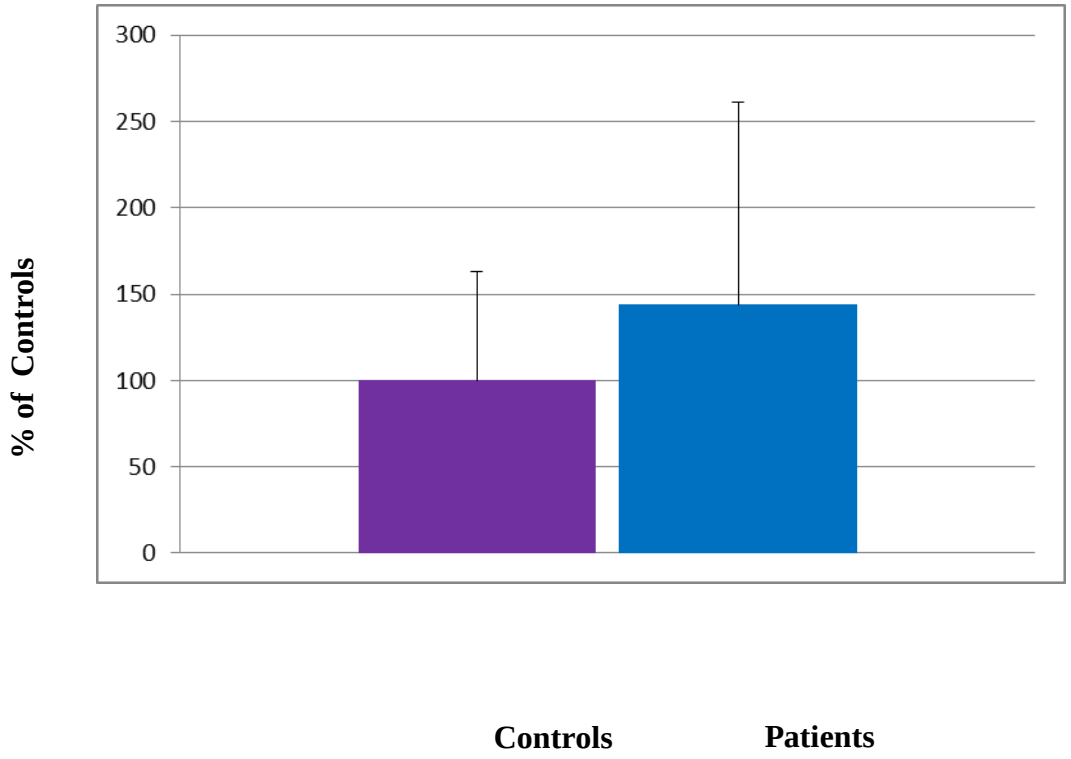
300
250
200
150
100
50
0
% of Controls
Controls
Patients

B

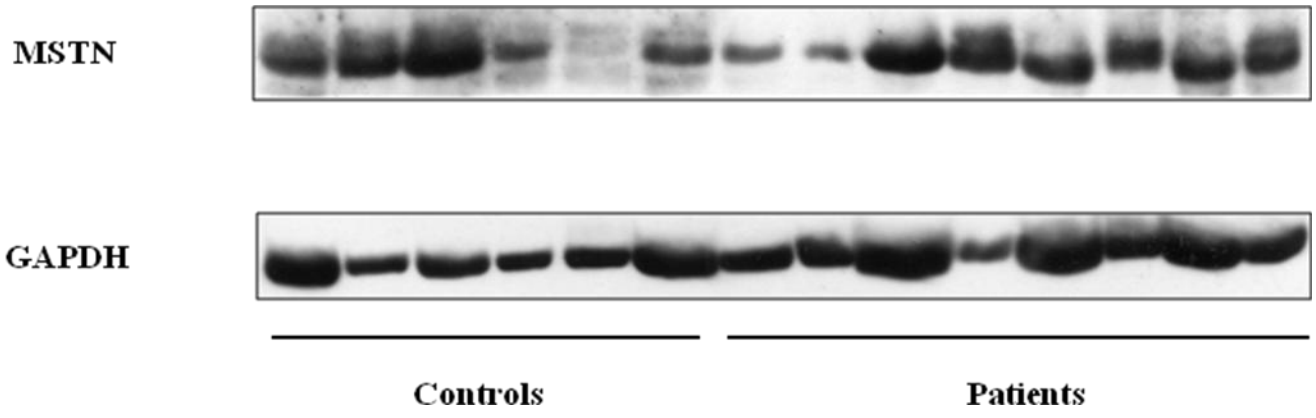
MSTN
GAPDH
Controls
Patients

Fig.3.

A

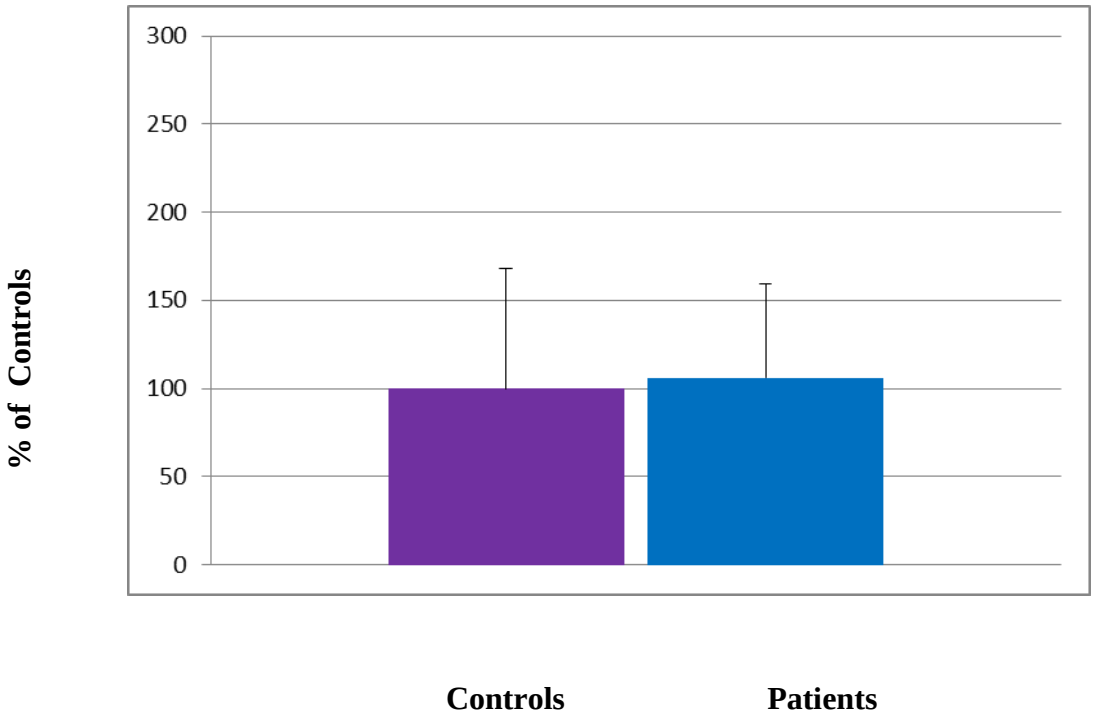
300
250
200
150
100
50
0
% of Controls
Controls
Patients

B

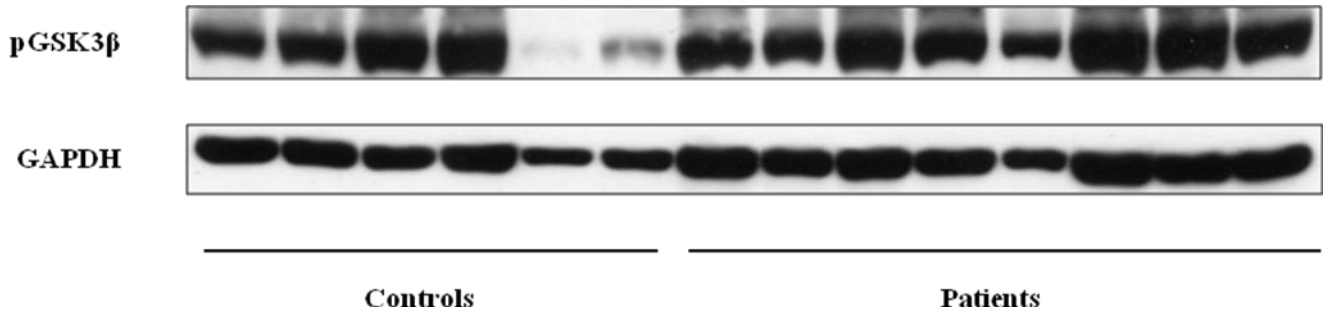
pGSK3β
GAPDH
Controls
Patients

Fig.4.

A

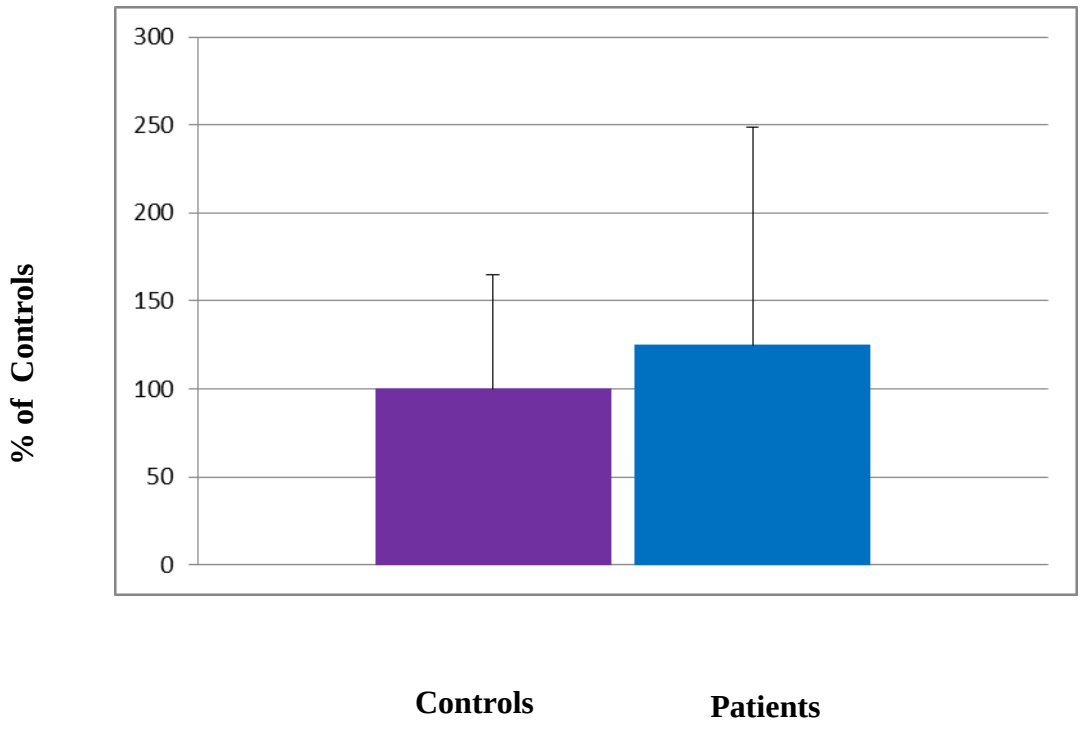
300
250
200
150
100
50
0
% of Controls
Controls
Patients

B

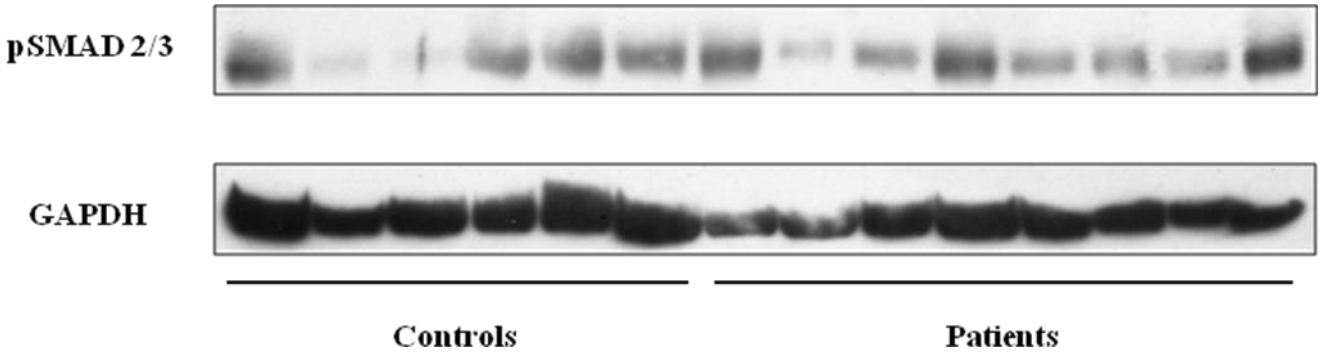
pSMAD 2/3
GAPDH
Controls
Patients

Fig.5.